

# STRAW-b (STRings for Absorption length in Water-b): the second pathfinder mission for the Pacific Ocean Neutrino Experiment

---

K. Holzapfel, <sup>a,1</sup> C. Spannfellner, <sup>a</sup> O. Aghaei, <sup>b</sup> A. Baron, <sup>b</sup> J. Bedard, <sup>b</sup> M. Böhmer, <sup>a</sup> J. Bosma, <sup>b</sup> N. Deis, <sup>b</sup> C. Fink, <sup>a</sup> C. Fruck, <sup>a</sup> A. Gärtner, <sup>c</sup> R. Gernhäuser, <sup>a</sup> F. Henningsen, <sup>d</sup> R. Hotte, <sup>b</sup> R. Jenkyns, <sup>b</sup> M. Karl, <sup>a</sup> Na. Khera, <sup>e</sup> Ni. Khera, <sup>f</sup> I. Kulin, <sup>b</sup> A. Lam, <sup>b</sup> T. Lavalley, <sup>b</sup> K. Leismüller, <sup>a</sup> L. Papp, <sup>a</sup> B. Pirenne, <sup>b</sup> E. Price, <sup>b</sup> T. Qiu, <sup>b</sup> I. C. Rea, <sup>g</sup> E. Resconi, <sup>a</sup> A. Round, <sup>b</sup> C. Rott, <sup>h,i</sup> A. Ruskey, <sup>b</sup> L. Ruohan, <sup>a</sup> K. Sasaki, <sup>b</sup> M. Tradewell, <sup>b</sup> M. Traxler, <sup>j</sup> D. Vivolo, <sup>g,k</sup> S. Wagner, <sup>b</sup> E. L. Winter, <sup>a</sup> M. Wolf, <sup>a</sup>

<sup>a</sup>Department of Physics, Technical University of Munich, Germany

<sup>b</sup>Ocean Networks Canada, University of Victoria, Victoria, British Columbia, Canada

<sup>c</sup>Department of Physics, University of Alberta, Edmonton, Alberta, Canada

<sup>d</sup>Department of Physics, Simon Fraser University, Burnaby, Canada

<sup>e</sup>Center for Advancing Electronics Dresden, Technische Universität Dresden, Dresden, Germany

<sup>f</sup>Department of Physics, Technical University Kaiserslautern, Kaiserslautern, Germany

<sup>g</sup>National Institute of Nuclear Physics, Complesso universitario di Monte Sant'Angelo, Napoli, Italy

<sup>h</sup>Department of Physics and Astronomy, University of Utah, Salt Lake City, USA

<sup>i</sup>Department of Physics, Sungkyunkwan University, Suwon, South Korea

<sup>j</sup>GSI Helmholtz Centre for Heavy Ion Research, Darmstadt, Germany

<sup>k</sup>Department of Mathematics and Physics, University of Campania "Luigi Vanvitelli", Caserta, Italy

E-mail: [kilian.holzapfel@tum.de](mailto:kilian.holzapfel@tum.de), [christian.spannfellner@tum.de](mailto:christian.spannfellner@tum.de)

---

<sup>1</sup>Corresponding author.

**ABSTRACT:** Since 2018, the potential for a high-energy neutrino telescope, named the Pacific Ocean Neutrino Experiment (P-ONE), has been thoroughly examined by two pathfinder missions, STRAW and STRAW-b, short for Strings for Absorption Length in Water. The P-ONE project seeks to install a neutrino detector with a one cubic kilometer volume in the Cascadia Basin's deep marine surroundings, situated near the western shores of Vancouver Island, Canada. To assess the environmental conditions and feasibility of constructing a neutrino detector of that scale, the pathfinder missions, STRAW and STRAW-b, have been deployed at a depth of 2.7 km within the designated site for P-ONE and were connected to the NEPTUNE observatory, operated by Ocean Networks Canada (ONC). While STRAW focused on analyzing the optical properties of water in the Cascadia Basin, STRAW-b employed cameras and spectrometers to investigate the characteristics of bioluminescence in the deep-sea environment. This report introduces the STRAW-b concept, covering its scientific objectives and the instrumentation used. Furthermore, it discusses the design considerations implemented to guarantee a secure and dependable deployment process of STRAW-b. Additionally, it showcases the data collected by battery-powered loggers, which monitored the mechanical stress on the equipment throughout the deployment. The report also offers an overview of STRAW-b's operation, with a specific emphasis on the notable advancements achieved in the data acquisition (DAQ) system and its successful integration with the server infrastructure of ONC.

**KEYWORDS:** Neutrino detectors; Cherenkov detectors; Photon detectors; Detectors for astroparticle physics; Particle tracking detectors

**ARXIV EPRINT:** [2310.16714](https://arxiv.org/abs/2310.16714)

---

## Contents

<b>1</b>	<b>Introduction</b>	<b>2</b>
<b>2</b>	<b>STRAW-b Concept and Instrumentation</b>	<b>3</b>
2.1	Standard Modules	3
2.2	LiDAR Modules	6
2.3	Muon-Tracker Module	8
2.4	PMT-Spectrometer Modules	8
2.5	Mini-Spectrometer Module	11
2.6	Wavelength-shifting Optical Module	11
2.7	Fast Signal Digitization	12
2.8	Art Installations	13
<b>3</b>	<b>Deployment</b>	<b>13</b>
3.1	Deployment Approach	14
3.2	Design Considerations	14
3.3	Qualification of the Module Mechanics	16
3.4	Deployment with Data Loggers	17
<b>4</b>	<b>Operation of the Instruments in STRAW-b</b>	<b>19</b>
4.1	Standardized Module	20
4.2	Cameras, Mini-Spectrometer, and LEDs	20
4.3	PMT-Spectrometer	20
4.4	Muon-Tracker	20
4.5	LiDAR	21
<b>5</b>	<b>Distributed Control System and Data Acquisition of STRAW-b</b>	<b>21</b>
5.1	Data Acquisition System	21
5.2	Integration into Oceans 2.0/3.0	22
5.3	Communication Management	22
5.4	Safety Control and Monitoring System	22
<b>6</b>	<b>A Software Package for the Data Analysis for STRAW-b</b>	<b>23</b>
<b>7</b>	<b>Summary and Outlook</b>	<b>24</b>

---

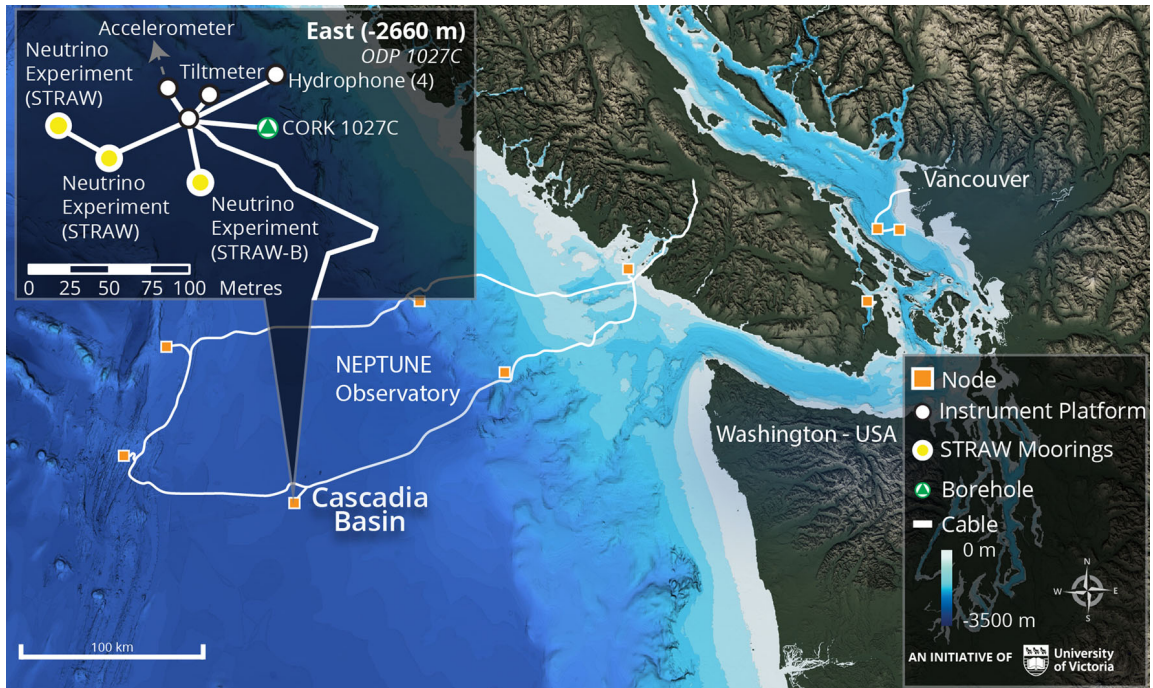


**Figure 1:** Maps of ONC’s NEPTUNE Observatory. P-ONE will be located at the Cascadia Basin node, where the pathfinder projects STRAW and STRAW-b have been until their recovery in July 2023. Image by courtesy of ONC.

## 1 Introduction

Astrophysical neutrino observations require additional neutrino telescopes on a cubic-kilometer scale alongside the operational IceCube detector [1–3]. Notable examples for such telescopes include KM3NeT (Cubic Kilometer Neutrino Telescope) [4], GVD (Gigaton Volume Detector) [5], and P-ONE (Pacific Ocean Neutrino Experiment) [6]. P-ONE is set to be situated within the Cascadia Basin, located off the shore of Vancouver Island, Canada, as shown in Figure 1. This initiative will leverage the existing deep-sea infrastructure, NEPTUNE, managed by ONC [7]. The project aims to instrument the ocean, spanning a 1 km height volume from the seafloor at 2660 m. Due to the challenging environmental conditions and the remote nature of the deep-sea location, a sturdy design for all components is imperative, along with comprehensive testing procedures.

Consequently, two pathfinder missions, namely STRAW and STRAW-b, short for Strings for Absorption Length in Water, have been deployed at the Cascadia Basin in 2018 and 2020 to investigate environmental parameters and feasibility for the cubic-kilometer scale neutrino detector [8, 9]. These missions are focused on investigating environmental variables and the viability of deploying a cubic-kilometer scale neutrino detector [8, 9]. While STRAW concentrated on assessing the optical characteristics of water in the Cascadia Basin [9], its successor, STRAW-b, employed cameras and spectrometers to examine the properties of bioluminescence [10–13] in the deep-sea environment.

## 2 STRAW-b Concept and Instrumentation

STRAW-b, the second pathfinder for P-ONE, was deployed in 2020 and situated approximately 40 m East of STRAW (see [Figure 1](#)). The primary motivation behind STRAW-b was to enhance our understanding of the expected background, explicitly focusing on bioluminescence. Additionally, it aimed to accumulate valuable experience for constructing and successfully deploying longer mooring lines required for extensive neutrino detector arrays.

The STRAW-b setup comprises ten modules mounted on a 444-meter-long mooring line, as illustrated in [Figure 2](#). With the exception of one module, all are enclosed in a 13-inch high-pressure-resistant glass housing. Each module is connected to its individual data cable providing network connectivity through glass fibers and power via copper wires. All cables are terminated at the mini junction box (MJB) located at the mooring's base [[14](#)].

### 2.1 Standard Modules

The instrumentation of STRAW-b followed a standardized module configuration, as shown in [Figure 3](#). The setup integrates electronics for power management, networking, and an Odroid C2 single-board computer [[15](#)]. The electronic elements are placed in the bottom section of the pressure housing, which consists of an aluminum plate and bowl. The compartment is illustrated in [Figure 2](#). To streamline the assembly process, the electronic components are securely attached to the aluminum plate, as depicted in [Figure 3](#). The aluminum plate is then connected to the aluminum bowl. The bowl, in turn, is affixed to the bottom of the glass pressure housing using optical gel as an adhesive. This configuration also functions as a heat sink for the electronic components [[14](#)].

Environmental sensors were added to monitor internal pressure, temperature, and humidity, serving as checkpoints for successful deployment and ongoing monitoring of the module's condition. To track the module's orientation and movements with the currents, an accelerometer and an electronic compass were employed. To manage and monitor individual electronic subcomponents, a total of six direct current (DC) supplies are utilized, each of which is configurable and capable of measuring voltage and current. Furthermore, each module is equipped with a battery-powered data logger designed to assess the environmental conditions during the deployment. The data recorded by these loggers is presented and analyzed in [Section 3.4](#) [[14](#)].

Expanding on this standardized configuration, certain modules incorporate specialized instruments tailored for specific measurements. These additional instruments are accommodated in the available space outside the electronics compartment, allowing for a modular and seamless integration. The following sections will offer an overview of these supplementary instruments.

To ensure a reliable system, a sophisticated electronic layout has been developed, particularly as it must be adaptable to the various different configurations and dimensions. The layout is shown as a simplified block diagram in [Figure 4](#). Data transfer and power connection between the modules and the MJB is provided by single hybrid cables with copper wires for power and two single mode fibres for communication. At the heart of the readout is the TRB3sc (see also [Section 2.7](#)), an integrated readout system based on a Field-Programmable Gate Array (FPGA) with central trigger system, slow control, Gigabit Ethernet and time-to-digital converter (TDC) [[16](#)]. This device was developed for collider experiments at GSI in Darmstadt and therefore benefits from experience and proven reliability [[16](#)]. The front-end of the TRB3sc is the so-called Padiwa, which amplifies

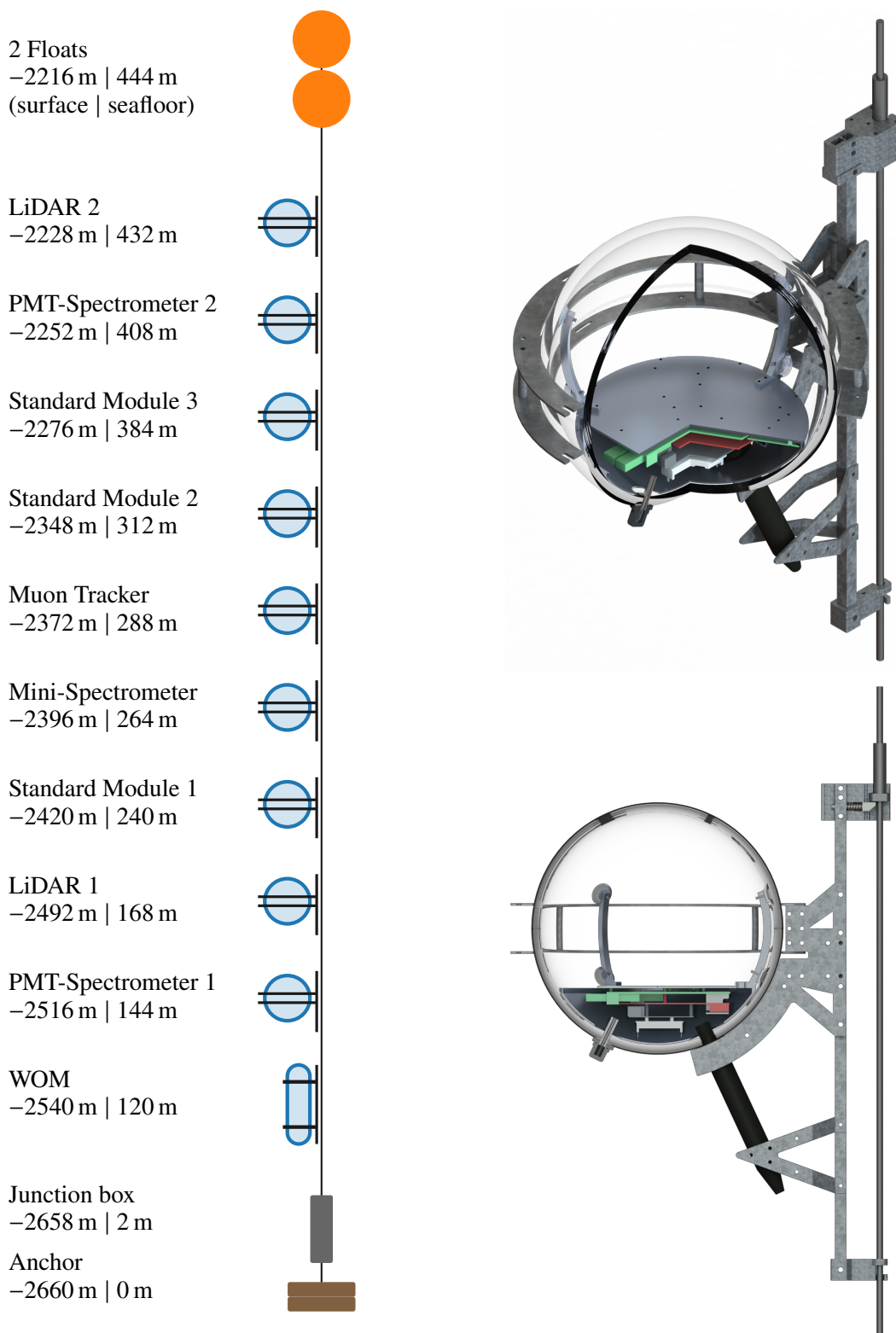


**Figure 2:** Illustration of the STRAW-b mooring line (left), and two cut views of the standardized module (upper and lower right) where the electronics compartment is visible.

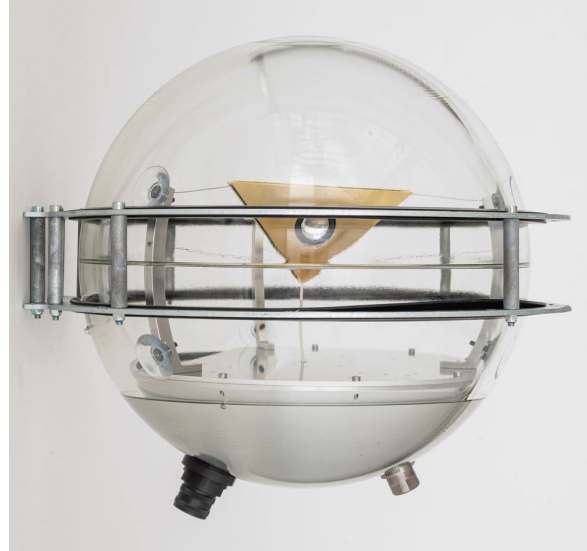
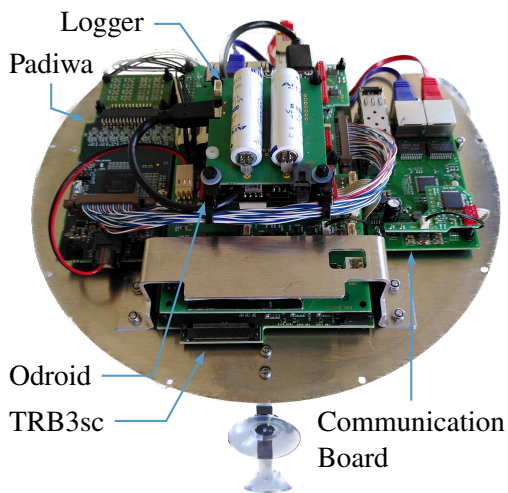


**Figure 3:** Standardized module electronic (left) and Standard Module 3 hosting the art & science installation *radioamnion* (right). The electronic components are positioned within the aluminum compartment located at the lower section of the pressure housing, while the upper part of the sphere is designated for the sensors of the specialized modules. The standardized module configuration is detailed in [Section 2.1](#).

and shapes the signal of the 16 inputs to allow a proper time-over-threshold measurement. The photosensor signal of each specialised module is fed to the Padiwa via the padAdap, a small adapter board. Communication with the devices is handled by an Odroid C2 [15]. The connection between the C2 and the TRB3sc is made by a carrier board called Phobos. The Phobos also contains power conversion via switchable DC-DC converters, as well as several digital-to-analogue converters (DACs) and analogue-to-digital converters (ADCs). It also hosts environmental sensors for pressure, temperature, humidity, acceleration and magnetic field, which are read by the Odroid via an I2C connection. Additionally, the power consumption of each DC-DC converter can be monitored via I2C. As the connection to the Odroid is based on Ethernet, a media converter is used as the interface to the fibre optic connection. A small add-on board replaces the microcontroller on the media converter, turning it into a configurable Ethernet switch. Port-based VLAN is implemented as a default configuration, isolating the TRB3sc Ethernet port from the small form-factor pluggable (SFP) uplink. This avoids congestion of the data links by hardware or software failures and ensures the accessibility of the module. [Figure 4](#) shows the general readout structure with the subsystems mentioned. In addition, a battery-powered data logger (Uboot) is housed in the modules to specifically record the acceleration and orientation of the instruments during deployment. A magnet attached to the glass housing must be removed just prior to deployment to switch a magnetic relay and initiate data acquisition by the Uboot. The data collected by the Uboot during the deployment is presented in [Section 3](#) [14].

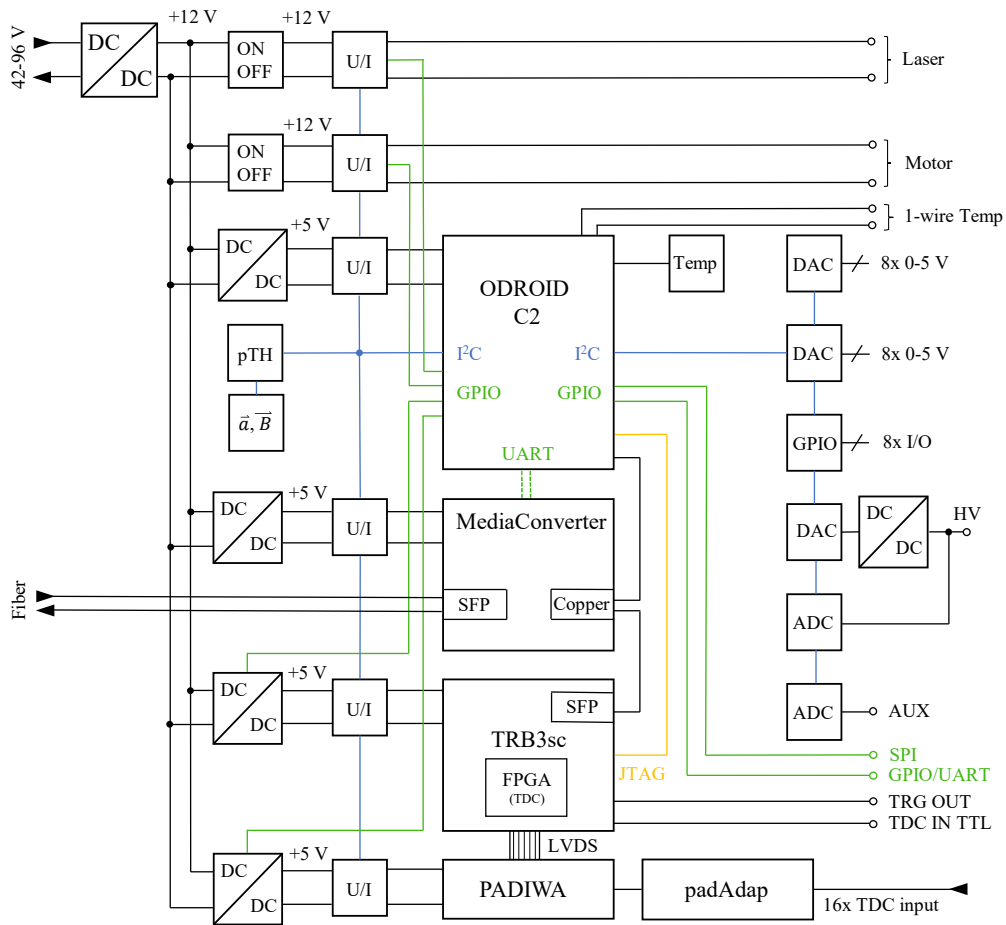


**Figure 4:** Simplified block diagram of the electronics for the standard module. Specific functions can be tailored to the respective modules by software modifications. For more information on the base electronics refer to the text.

## 2.2 LiDAR Modules

Two light detection and ranging (LiDAR) modules aim to verify the attenuation length measurements from STRAW and separately determine scattering and absorption length. These are equipped with a pulsed laser diode as an emitter, while a lens focuses the back-scattered photons onto a micro photomultiplier tube (PMT) device to measure intensity over time. A complete assembly of the internal LiDAR components is depicted in [Figure 5](#). The procedural steps of the measurement are outlined below.

An electric trigger signal initiates the emission of a  $(450 \pm 10)$  nm light pulse by a laser diode (NPL45B) [17]. The light pulse is emitted after a delay of approximately 35 ns [17] to the trigger, which is operated at 10 kHz. The laser is configured to the shortest available pulse width of  $(5 \pm 1)$  nm FWHM (full width at half maximum) [17]. The back-scattered photons are then detected by a micro PMT H12406 from Hamamatsu [18]. To limit the PMT to mainly detect the laser's light, a filter  $(450 \pm 10)$  nm and a 1" lens is used. The lens also enhances the light sensitivity to the laser



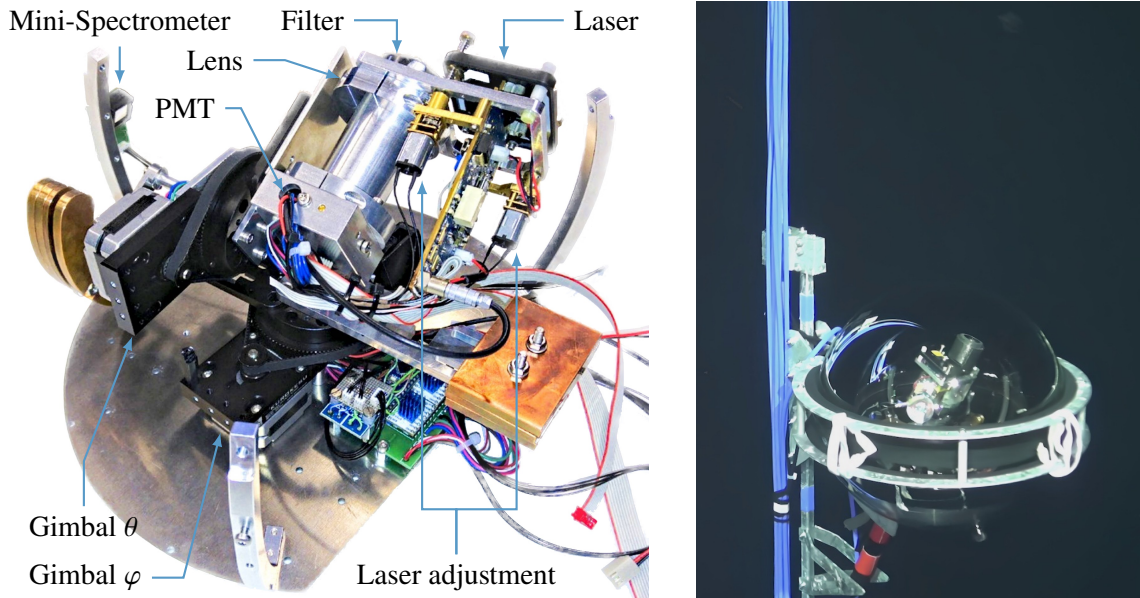


**Figure 5:** Picture of the internal LiDAR components (left) and during an inspection dive with a remotely operated vehicle (ROV) (right). In the image of the inspection (right), the LiDAR is pointing towards the upper right. Further information about the module is elaborated upon in [Section 2.2](#).

beam. Furthermore, the laser's intensity is set to a level where the PMT detects with approximately 50 % at least one photon per pulse. The micro PMT H12406 has an internal counting electronic that provides an electric signal of 20 ns for each detected photon with a delay of 6 ns including the transit time spread (TTS) [18]. The laser trigger and PMT's electric signals are digitalized by a Trigger Readout Board (TRB) [16], as outlined in [Section 2.7](#). The TRB has a sub-nanosecond timing precision and provides two timestamps for each detected photon: the time of the laser trigger and the time delay from the laser trigger to the PMT's signal. These two values are critical for LiDAR measurements, enabling the analysis to determine the number of detected photons per laser pulse and the time of flight of each detected photon [14, 19].

The laser, filter, lens, and PMT are affixed to a rotation stage featuring two axes. This configuration permits adjustments to the orientation in azimuth and zenith. Furthermore, two motors enable alterations to the laser's pointing direction, ensuring precise alignment with respect to the field of view (FoV) of the PMT [14, 19].

The LiDAR is equipped with an in-situ laser calibration system. To achieve this, the gimbal is positioned in a specific manner, allowing the laser to illuminate both a pin-diode and a C12880MA mini-spectrometer from Hamamatsu [20] simultaneously. This mini-spectrometer corresponds to the type employed in the Mini-Spectrometer and PMT-Spectrometer modules. Through this configuration, it becomes possible to measure both the spectrum and the intensity of the laser during its lifetime in the deepsea [14, 19].

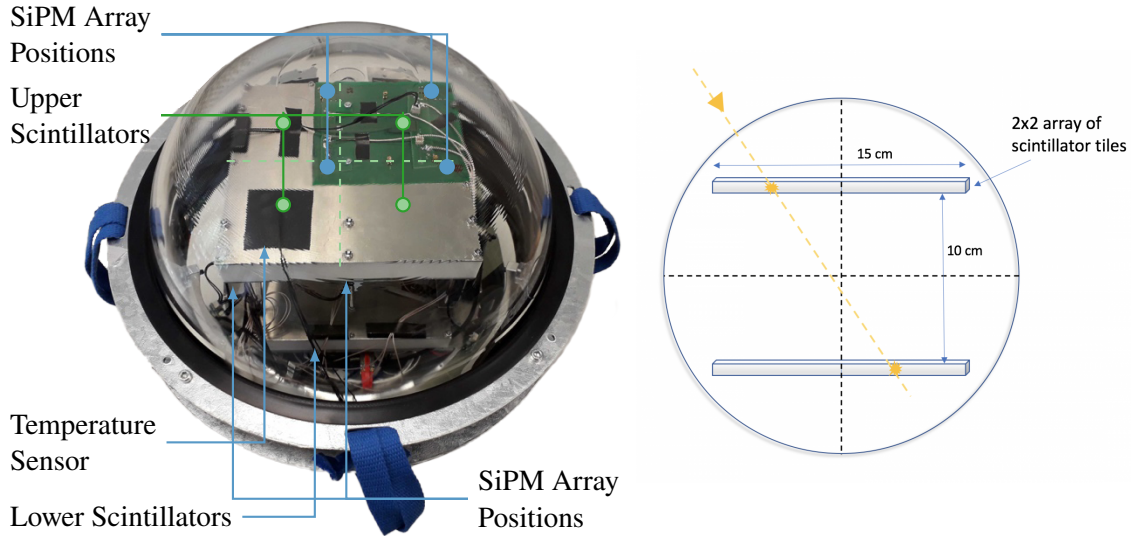


**Figure 6:** Picture of the Muon-Tracker module (left) and sketch with a muon track interacting in the two scintillator arrays (right). Further information about the module is elaborated upon in [Section 2.3](#).

### 2.3 Muon-Tracker Module

One Muon-Tracker module, depicted in [Figure 6](#), is devised to detect muons within the confined module volume. This detection holds particular significance, as it can function as a calibration instrument, validating pointing resolution for large-scale neutrino detectors such as P-ONE. Upon measuring a muon, the device imposes a constraint on the muon’s trajectory, necessitating it to traverse the module. This information can then be juxtaposed with the reconstructions derived from Cherenkov light data of the neutrino detector [[14](#), [21](#)].

The module employs eight BC-404 plastic scintillator tiles [[22](#)] organized in two 2x2 arrays, positioned vertically at a separation of 10 cm, as illustrated in [Figure 6](#). Each individual scintillator tile measures 75 mm × 75 mm × 20 mm in dimension. Within the 2x2 array configuration, the scintillator tiles are divided by Teflon walls of 6 mm thickness [[21](#)].

When a muon traverses the scintillator, it emits light across a broad spectrum that reaches its peak at 408 nm [[22](#)]. Two 3x3 matrices of KETEK PM3315-WB-B0 silicon photomultipliers (SiPMs) [[23](#)] measure the induced light in each scintillator tile at diagonal corners. The purpose of the 3x3 matrix is to enhance the coverage of the sensitive area, and within each matrix, the nine SiPMs are linked in parallel to a single readout channel. In instances of time-correlated events occurring within separate scintillator tiles, an approximation of directional information can be derived. The 16 channels of SiPM signals are digitized using a TRB [[16](#)] and Padiwa [[24](#)], a methodology akin to other modules. The system of TRB and Padiwa is described in [Section 2.7](#) [[14](#), [16](#), [21](#), [24](#)].

### 2.4 PMT-Spectrometer Modules

Two PMT-Spectrometer modules, illustrated in [Figure 7](#), are characterizing the bioluminescence emissions. Within each module, three distinct sensor types are accommodated: twelve PMTs serv-

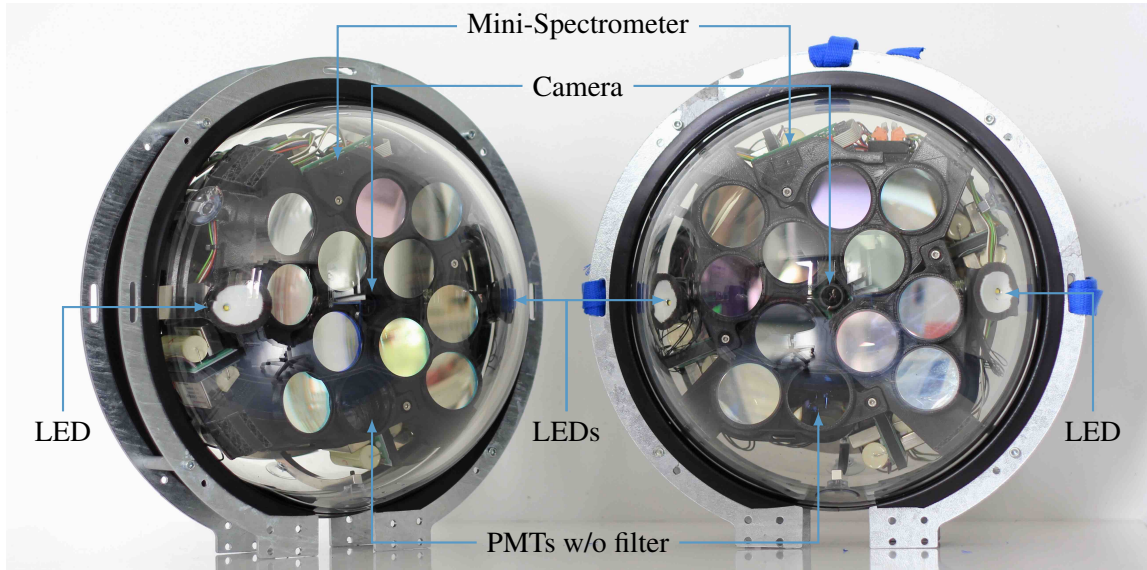


**Figure 7:** The two PMT-Spectrometers post-assembly, featuring distinct sensor labeling. Circular mirrors represent the filters. Further details regarding the components and measurement principles are expounded in [Section 2.4](#).

ing as a spectrometer, a low-light color CMOS camera [25, 26], and a C12880MA mini-spectrometer from Hamamatsu [20]. These sensors collectively enable three separate and independent bioluminescence measurements, each offering its unique benefits. All sensors are oriented upwards within the deployed modules to achieve an overlapping field of view [14, 27, 28]. Subsequently, a more detailed discussion of the individual sensors follows.

Each of the twelve 1" PMTs [29, 30] is paired with its own individual 2" lens [31] and 2" wavelength filter [32–34]. The individual PMTs are deliberately separated from one another in terms of optics. The arrangement of these twelve units varies in position and angles concerning the module's vertical axis. This specific configuration counteracts the distortion caused by the spherical pressure housing of the modules while optimizing the overlapping FoV for all PMTs. The arrangement was devised through a Geant4 [35, 36] simulation, which was instrumental in determining the most advantageous positioning of these components. Given the complexity of the configuration and the constraints on available space, a 3D-printed holding structure was used to maintain the designated position of the components. Before the light reaches a PMT, it initially passes through hard-coated OD 4.0 bandpass filters [32–34]. These filters possess distinct center wavelengths (CWLs) within the range of 350 nm–525 nm [27, 37]. It is important to note that one PMT is devoid of a filter to monitor integrated intensity. Following the filter, the light propagates through an LA1401-A lens with a focal length of  $59.8 \text{ mm} \pm 1\%$  and a diameter of  $50.8_{+0.0}^{-0.2} \text{ mm}$  [31], which effectively focuses the light onto the PMT. Two distinct types of PMTs [29, 30] are employed in order to harness their different spectral responses, where the R1924A PMT is utilized in conjunction with filters for wavelengths of 510 nm and below, as summarized in [Table 1](#). Positioned at a distance of 30 mm beyond the lens, the PMT is situated at approximately half the focal length. This configuration ensures the projection of a point source onto roughly half of the PMT's photocathode area. As a result, each PMT captures a distinctive spectral segment of an emission.

**Table 1:** Summary of 12 color channels of the PMT-Spectrometer with the parameters of the filters and the type of PMT [29, 30, 32–34].

Lens					Lens				
CWL <sup>1</sup>	FWHM <sup>2</sup>	TP <sup>3</sup>	Part	PMT	CWL <sup>1</sup>	FWHM <sup>2</sup>	TP <sup>3</sup>	Part	PMT
[nm]	[nm]	[%]	number	type	[nm]	[nm]	[%]	number	type
350.0	50.0	≥95	12-099	R1924A	480.0	10.0	≥85	65-206	R1924A
400.0	25.0	≥90	86-664	R1924A	492.0	10.0	≥85	65-209	R1924A
425.0	25.0	≥90	87-799	R1924A	510.0	10.0	≥85	65-213	R1924A
450.0	10.0	≥85	65-201	R1924A	525.0	25.0	≥90	87-801	R1925
460.0	10.0	≥85	88-016	R1924A	550.0	25.0	≥90	86-667	R1925
470.0	10.0	≥85	65-205	R1924A	integrating channel without filter				R1925

<sup>1</sup>CWL: Center Wavelength

<sup>2</sup>FWHM: Full Width at Half Maximum

<sup>3</sup>TP: Transmission Peak

Combined, these segments seamlessly unveil the complete spectrum of a bioluminescence emission, offering a remarkably higher sensitivity compared to the other two sensors. The signals from the 12 PMT channels are transformed into digital data through the employment of a TRB [16] and Padiwa [24] readout as described in Section 2.7 [27].

The low-light camera is a custom-designed device, initially developed in partnership with Arducam for applications in the IceCube Upgrade and IceCube Gen2 [25, 26]. This choice was motivated by the potential synergies across neutrino detectors, which necessitate hardware capable of functioning in remote locations with space constraints, low power consumption, and under low-light conditions [25]. Central to the camera’s design is the IMX225LQR-C CMOS image sensor [38, 39], featuring a resolution of 1312 x 979 pixels and incorporating an RGB color filter array (CFA), often referred to as a Bayer Filter [40]. Optically, the camera utilizes an Arducam lens, specifically the M25170H12 model, with a FoV of approximately 170° [26, 41]. In order to further augment the camera’s capabilities, an integrated LED system has been introduced into STRAW-b. For each camera in the PMT-Spectrometer modules, a total of six LEDs are incorporated. Within this set, two white LEDs [42] are positioned in close proximity to the camera itself, as illustrated in Figure 7. The remaining four LEDs are strategically located in the adjoining LiDAR modules, which are situated 24 m above the PMT-Spectrometer modules, falling within the shared field of view of both the camera and the PMTs. Each LiDAR module incorporates two sets of white [42] and ultraviolet (UV) [43] LEDs, with one set oriented downwards and the other set directed horizontally [28].

Furthermore, the module is also equipped with a C12880MA Mini-Spectrometer [20], akin to the configuration present in the Mini-Spectrometer module. Detailed information about this module and the C12880MA spectrometer is presented in the subsequent Section 2.5 [27].

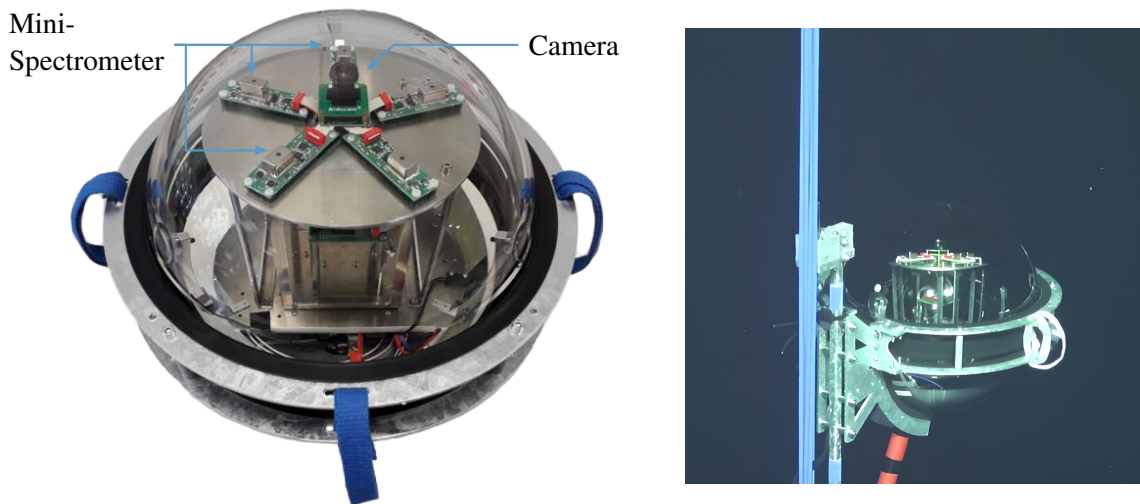


**Figure 8:** Picture of the Mini-Spectrometer Module (left) and during an inspection dive with a ROV (right). The Mini-Spectrometer Module accommodates a camera and five C12880MA Mini-Spectrometers. Further information about the module is elaborated upon in [Section 2.5](#).

## 2.5 Mini-Spectrometer Module

The Mini-Spectrometer module is composed of five C12880MA Mini-Spectrometers [20] and a low-light camera, as depicted in [Figure 8](#). Both components are identical to the ones utilized in the PMT-Spectrometer module. The Mini-Spectrometer is a complementary device to the spectrum measurement of the PMT-Spectrometer and the cameras. It allows to measure finer resolved spectra than the PMT-Spectrometer and camera but has a lower light sensitivity. In order to offset this reduced sensitivity, the module incorporates a total of five Mini-Spectrometers. These Mini-Spectrometers are symmetrically arranged around the centrally located camera. Additionally, both the Mini-Spectrometers and the camera have their FoV oriented upwards [14, 20, 44].

The measurement principle of the Mini-Spectrometer is outlined in this paragraph. The incoming light, passing through a 0.5 mm entrance slit with a numerical aperture of 0.22, is focused by a collimating lens onto a grating chip. This grating is responsible for dispersing the incoming light into its spectral components at specific diffraction angles. The grating, combined with the chip's curvature, leads to creating an image where wavelengths are arranged linearly across the image sensor. The C12880MA Mini-Spectrometer uses a complementary metal-oxide-semiconductor (CMOS) image sensor with 256 pixels to digitizes the intensities of the detected light. These pixels correspond to a spectral range spanning from 340 nm–850 nm, providing a FWHM resolution of less than 15 nm [20].

## 2.6 Wavelength-shifting Optical Module

The Wavelength-shifting Optical Module (WOM) [45] is a photosensor instrument, designed to enhance the sensitivity of large detector volumes with single-photon detection capability. The key objective is to improve the signal-to-noise ratio, which is achieved by decoupling the photosensitive area from the cathode region of its PMT. The WOM comprises a transparent tube housing two PMTs

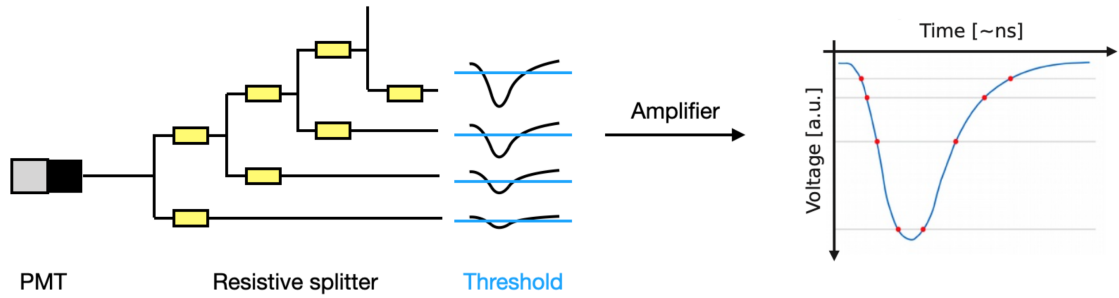


**Figure 9:** Simplified measurement principle for the time-over-threshold measurement. The red marked positions in the left plot are the timestamps stored by the TRB with sub-nanosecond precision. For more information on the base electronics refer to the text.

on its ends. Coated with wavelength-shifting paint that efficiently absorbs ultraviolet photons, the tube can capture and guide up to 73 % (41 % in ice or water) of subsequently emitted optical photons via total internal reflection towards the PMTs. A prototype of the WOM, tailored for application in the IceCube Upgrade and IceCube Gen2 projects, was deployed as the lowermost module along the STRAW-b mooring line [45].

## 2.7 Fast Signal Digitization

LiDAR, PMT-Spectrometer, and Muon-Tracker utilize a TRB (version TRB3sc) [16] to digitise signals from PMTs or SiPMs where nanosecond precision is required. The TRB can be used to perform a time-over-threshold (ToT) measurement as shown in Figure 9. The TRB has a 16 channel time-to-digital converter (TDC) that measures the rising and falling edges of a trigger signal with sub-nanosecond precision. The TDC is performed by firmware on a FPGA. To convert an analogue signal into a trigger signal, other electronic components are required, such as the Padiwa [24]. The Padiwa is a 16-channel discriminator board designed to enable ToT measurement with the TRB. It uses a discrete analogue stage to amplify the incoming signal, followed by a secondary slow shaping stage that allows the application of thresholds to the ToT trigger signal. The thresholds can be configured individually for each channel, with a precision of 16 bits.

An advantage of the TRB’s measurement principle, with respect to full signal digitization, is effective data reduction while preserving a high time resolution [16, 24]. Furthermore, the TRB system allows the detectors to operate in two modes: high-precision and low-precision. In the high-precision mode, the exact timestamp of each pulse is recorded with sub-nanosecond precision relative to the master clock, enabling analysis at the single-photon level. In contrast, the low-precision mode records only the number of pulses within a specified time interval similar to a scaler [16].

Storing the TRB data for long-term monitoring is not always feasible due to the large data size it generates (up to 100 MB per minute). Therefore, the DAQ operates in the low-precision mode where only the signal’s threshold transgressions are counted. The counters are then recorded at a frequency of 1 kHz.

The signals of the SiPMs and PMTs in the Muon-Tracker and PMT-Spectrometer, respectively, are digitized with the Padiwa, where the thresholds are set at an appropriate level to achieve

sensitivity to single photons. The LiDARs are using a photon counting base for the PMT, which provides a trigger signal directly without a Padiwa. Furthermore, the LiDAR and Muon-Tracker operate in high-precision mode since both require sub-nanosecond precision, and the dark rates are optimized to a few Hz, allowing long-term monitoring in high-precision mode. In contrast, the PMT-Spectrometer operates in low-precision mode to compress the kHz to MHz signal effectively.

## 2.8 Art Installations

In addition to its scientific objectives, specific modules of the project also serve as hosts for art installations created in collaboration with the Sonderforschungsbereich 42 (SFB42) [46], a research group of artists and physicists based in Munich. This collaborative project, known as *UNDERCURRENTS* [47], involves a group of artists from the Fine-arts Academy in Munich to facilitate a creative partnership between the two disciplines which can turn science into captivating art and forge a deeper public understanding of P-ONE and science, in general [48]. As one result, the sound art project *radioamnion* [49] was developed, built, and integrated in the Standard Module 3, as depicted in Figure 3. During each full moon, *radioamnion* broadcasted sonic transmissions of invited artists.

## 3 Deployment

As deployment, we describe the procedure of bringing a detector structure from a ship to the sea and placing it on the sea floor at its foreseen location [50]. For STRAW-b, it also includes the subsequent connection to the NEPTUNE network [7, 51].

Deployments in the deep-sea presents a variety of challenges that stem from the unique, remote, and challenging environment of the ocean depths. The process involves overcoming significant logistical hurdles, as accessing and operating equipment at great depths is inherently complex. The extreme water pressure, low temperatures, and corrosive nature of seawater require the development of specialized materials and robust engineering to ensure the durability of the detectors [50, 52]. Additionally, the remote and inaccessible nature of deep-sea locations poses difficulties in deployment and maintenance. Unlike surface installations, where repairs and adjustments can be readily performed, the deep-sea offers limited opportunities for intervention due to its inaccessibility and the high cost associated with underwater operations. Moreover, the light absorption within the water introduces an additional level of complexity, requiring cable connections to provide both power and communication capabilities for the detectors. Overcoming these challenges demands a multidisciplinary approach, combining expertise in marine engineering, materials science, and particle physics [50, 52].

Full-scale neutrino detectors are especially complex as the targeted instrumentation volume is on the scale of one cubic kilometer or larger [53]. First endeavours of deep-sea neutrino telescope installations were made by the DUMAND project [54, 55] in the Pacific Ocean. Years after, deep-sea neutrino experimentation predominantly occurred in the Mediterranean Sea, with detectors such as ANTARES [56, 57], NESTOR [58], NEMO [59–62], and KM3NeT [53, 63]. In 2008, ANTARES, NESTOR, and NEMO collaborated to establish and operate the cubic kilometer-scale KM3NeT, pooling their resources to tackle the inherent complexities [53]. Despite the passage of 16 years, no readily available technology exists for the direct construction of other detectors due

to the intricate challenges involved. Consequently, the STRAW-b initiative aims to accumulate valuable experience in preparation for the P-ONE project [6].

### 3.1 Deployment Approach

Deployments of instrumented mooring lines can be categorized into two primary approaches: top-down and bottom-up [50]. The bottom-up method involves placing an enclosed structure on the ocean bed and unfolding the mooring line through release mechanisms and its buoyancy. On the other hand, at top-down procedures, the mooring line is lowered from the sea surface to the seabed, typically with a heavy lift line from a deployment vessel. In top-down approaches, the deployment order can be anchor first or buoy first, referring to the part initially deployed from the ship [50].

When using a buoy first approach, the mooring line must first be expanded on the sea surface, increasing the deployment time [50]. Conversely, anchor-first deployments place greater mechanical stress on both the mooring line and the equipment, as the mooring line is responsible for supporting the weight of the anchor throughout the operation. Unfavorable sea conditions can escalate this strain further, necessitating a winch with appropriate load rating on the ship and increasing overall handling complexity. Apart from the deployment method, several other factors must be considered during the process. The sea state, wind speed, and swell are crucial as they impact the positioning of the deployment vessel, as well as the handling of deck work by the crew, and the impact on scientific instrumentation. Therefore, the deployment procedure must account for these factors and adapt to changing weather conditions, even if tailored to a specific sea state. Typically, deployment operations are scheduled during daylight hours with a stable weather window of at least 12 hours [50]. However, marine operations and equipment handling must be designed to withstand the anticipated loads and sea conditions while ensuring practicality and safety [50, 52].

In the case of STRAW-b, a buoy-first deployment was chosen based on a combination of factors, including the available deck space and winches on the ship, as well as the design considerations detailed in Section 3.2. Additionally, this approach enables the crew to provide enhanced protection for the delicate instruments by minimizing contact with the ship, as the steel line is under less tension compared to an anchor-first method.

### 3.2 Design Considerations

The STRAW-b project was designed around 14 existing deep-sea cables that were provided from a previous experiment. These hybrid cables are composed of copper wires for power and fiber elements for data transmission, and have been terminated with a dry-mate connector with a length of approximately 20 cm. This design, however, is sub-optimal for the used instrument pressure housing made from glass. The lever arm created by the long connector posed a significant threat to the integrity and durability of the systems. As part of the risk mitigation, a buoy-first top-down deployment procedure was chosen, allowing immediate response by the deck crew during the deployment procedure. The hybrid cables started with a length of 120 m and increased in steps of 24 m up to a maximum size of 432 m. Each of the ten deployed instruments has been connected with its own hybrid cable to the MJB, resulting in a star-like network topology. The remaining four connection cables were used for testing.

The modules, connected to their respective hybrid cable, are stored on an instrument tray (Figure 10), while the steel line is separately stored on an electric winch. The two components are



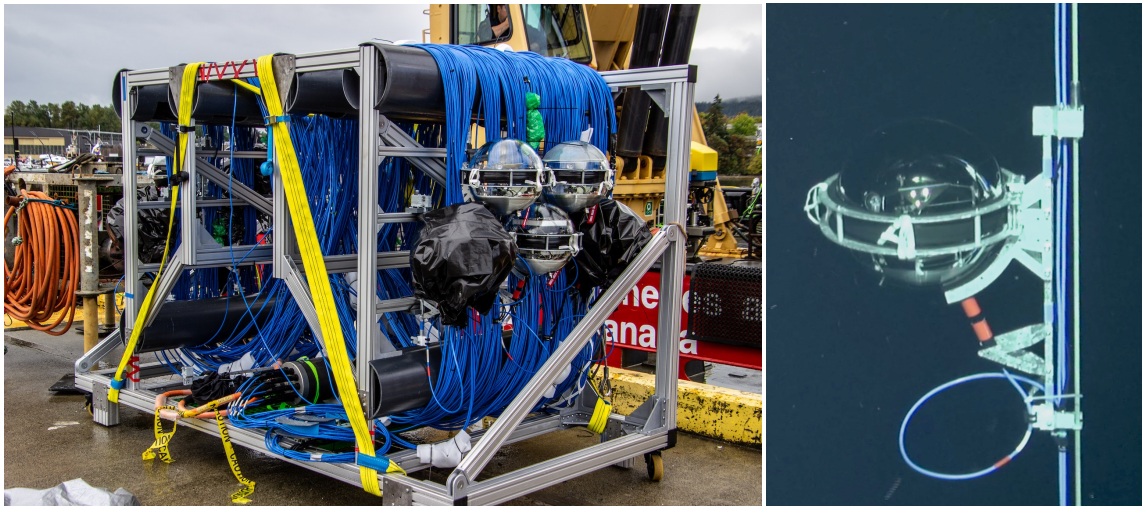


**Figure 10:** Images of the instrument tray with affixed modules (left) and a deployed module (right), captured during the initial inspection dive of a ROV following the successful deployment.

joined together during deployment on the back deck before going overboard. The mating between the two occurs using a specially designed 'click-in' mechanism with ferrules on the steel line.

The STRAW-b module mounting must be a complement to these ferrules, while providing also a secure fixation of the glass sphere without obstructing the field of view of the upper hemisphere. Additionally, the external mounting must be lightweight, as the modules need to be handled during the offshore operation. In addition, the aforementioned difficulties caused by the length of the inherited dry-mate connector had to be taken into account. Several design iterations and module mounting prototypes were required to meet all these requirements. In the end, the design shown in [Figure 10](#) was chosen. Most of the components are laser and water-cut steel parts that can be manufactured in a time and cost efficient manner. The mounting principle of the sphere is based on two steel rings located 30 mm above and below the equator. This ensures that the sealing and adhesive tapes are not affected by mechanical stress. The rings were designed with a small gap between the glass and the steel, which was eventually filled by an ethylene-propylene-diene monomer (EPDM) rubber edge protector. EPDM is a seawater resistant synthetic rubber [64]. The external mounting relies on the squeezing of the rubber band to exert sufficient pressure on the sphere to hold it firmly in place. The EPDM rubber is strong enough to protect the glass from damage [14].

The other important aspect of the mounting is the click-in mechanism for the cable ferrules. This is achieved by using a stack of four 12 mm thick steel plates with different recesses to follow the shape of the ferrule. The basic design is shown in [Figure 11](#). By using a compression spring and a steel slider, similar to a door lock, the ferrule can be clicked into the mechanism. The sub-components of the external mounting are connected by a square profile. One of the holes in the profile is used as a stop for the compression spring. The square profile has a total length of 650 mm to accommodate the dimensions of the glass sphere and the attached connector. However, as the sphere is offset from the steel cable, it is necessary to prevent the module from tilting. Two small hooks are therefore located at the bottom of the bracket. By rotating the module orthogonally to the

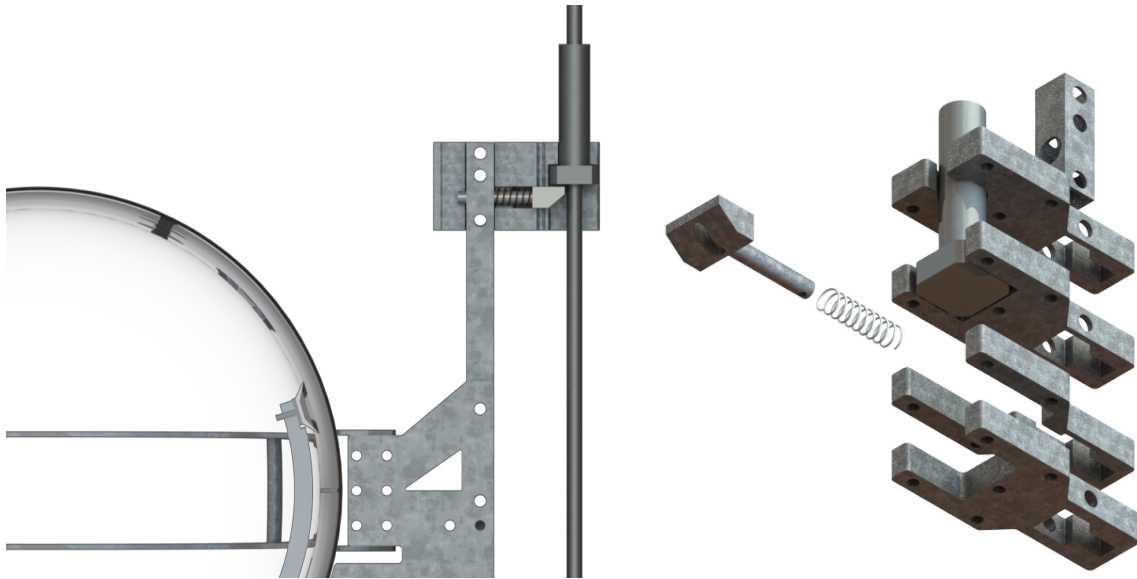


**Figure 11:** Exploded view of the click-in mechanism (left) and cutaway view when connected to the ferrule on the steel line.

bearing steel cable, they can be hooked into and the module can be rotated again to lock the ferrule. As this has to be done on the deck of the support vessel, the mounting had to be lightweight. The total weight of the mount was reduced to around 5 kg by using recesses and struts rather than full metal parts. The strain on the hybrid cable is reduced by a double system: the connector attached to the sphere has static strain relief by means of a cable clamp, while the remaining bundle of cables has a degree of freedom by means of a bungee cord. The maximum elongation of the bungee cord prevents damage to the hybrid cable and connector in the event of increased stress, even when submerged. Protective plates under the ball further protect the connector from mechanical shock. The plates are designed in a triangular shape to allow the bungee cord to slip and prevent knots when the cord is not under tension [14].

### 3.3 Qualification of the Module Mechanics

To address the challenges associated with the STRAW-b modules, risk mitigation measures have been implemented through a series of tests. These tests specifically focused on evaluating the modules' resistance to environmental conditions in the deep-sea and the stresses encountered during deployment. They were conducted in alignment with standards and recommendations applicable to submarine infrastructure to ensure compliance and reliability [50, 52].

The drag caused by sea currents and the speed of descent during deployment can cause vibration in the instruments, with the potential to damage both electronics and mechanics [28, 50, 52]. Vibrations and shocks can also occur during transport and general handling of the equipment. For this reason, vibration and shock tests were carried out on a standard module and a prototype of the PMT spectrometer module in accordance with the ISO 13628-6 standard [52]. The test includes a sinusoidal vibration for each spatial axis with an amplitude of 2 mm for the frequency range 5-25 Hz and  $5 g_0$  ( $1 g_0 = 9.81 \frac{m}{s^2}$ ) between 25-150 Hz. Shocks with an acceleration of  $10 g_0$  are applied eight

times per direction [52]. Resonance searches within the tested frequency range of 5-150 Hz were also performed before and after the actual tests. Both modules were tested with the external mount, but the square rod and click-in mechanism had to be replaced with an adapter for the test table. Both units passed the test, as did the included readout electronics. The only observed problem was the loosening of four screws at the interface of the readout electronics to the internal mounting plate in one module. This issue was solved in the final design with longer screws and additional use of screwlock [14].

The pressure in the deep-sea has to be handled by the submersible instruments. For the Cascadia Basin, a pressure of roughly 270 bar is expected at a depth of 2660 m. The glass spheres used are already pressure rated, but their behaviour can be altered by adding specific holes, e.g. for bulkhead connectors. For this reason, a separate pressure test was carried out for a module assembly. The enclosure manufacturer Nautilus provides a special pressure chamber [65] for this purpose. Here the unit is repeatedly cycled to a maximum pressure of 375 bar, before the pressure is held for several minutes. The same module assembly was used for the pressure test as for the vibration and shock tests. The module passed the test successfully, although small detachments of the optical gel from the aluminium shell were observed. However, these quickly disappeared as the vacuum in the module was reduced and are not considered to be relevant to the behaviour of the instrument [14].

Between the end of December 2019 and the end of January 2020, a STRAW-b module was subjected to a long-term test. It was immersed in a test pool while pressure, temperature and humidity were monitored. The pool was filled with artificial seawater to investigate possible effects on the sealing of the module and connector. Throughout the test period, load resistors were used to simulate a working module. The internal pressure remain fairly stable at around 275 mbar. A steady decrease in humidity was also observed, most likely due to condensation as the module was not purged with nitrogen. Finally, no leakage was detected [14].

### 3.4 Deployment with Data Loggers

In order to quantify the stress on the equipment during deployment, a battery-powered logger was installed in each module, except the WOM, to assess this process in detail. This logger recorded various parameters including module acceleration, compass heading and internal conditions such as temperature, pressure and humidity. It began recording data after a magnet attached to the instrument casing was removed just before the start of the deployment. The data collected can serve as a valuable reference for future instrument design and testing. Figure 12 shows the data from three loggers. The figure includes markers (A-L) corresponding to specific events covered in the following description.

The deployment procedure commences by attaching three floats to the upper section of the steel line and extending the mooring horizontally on the sea's surface behind the ship, utilizing both currents and a Rigid-Hulled Inflatable Boat (RHIB). As the steel line is being unspooled, the modules, along with the hybrid cables, are connected to the line on the ship's rear deck. The first connected module is the LiDAR 2, while Figure 12 (A-E) symbolizes the connection of the MuonTracker, Mini-Spectrometer, LiDAR 1, and PMT-Spectrometer 1, respectively. After a module is connected, it is carefully guided into the water to avoid any contact with the boat. The MJB is then affixed to the line (F), followed by disconnecting the line from the winch (G) to mount the anchor. Upon releasing the anchor (H) from the ship's deck, the string aligns vertically and floats freely in

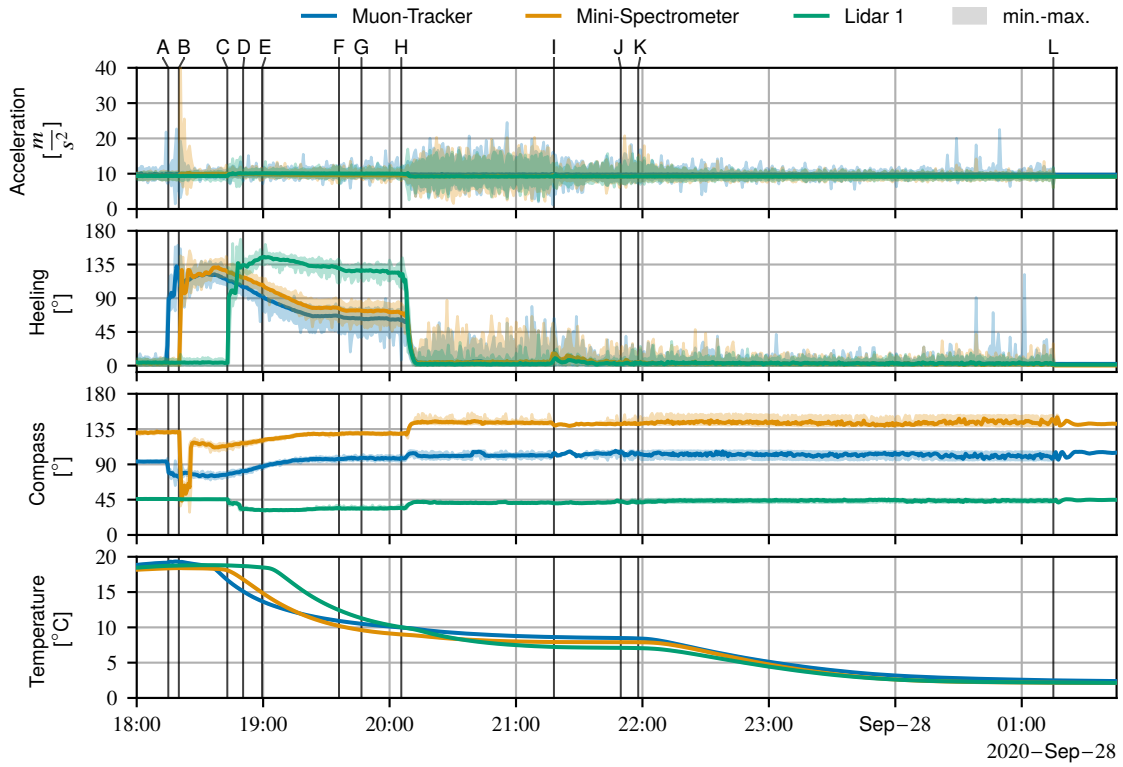


**Figure 12:** Data obtained from the deployment logger of three modules. The three modules get connected to the string in the order Muon-Tracker, Mini-Spectrometer, and LiDAR 1, indicated as (A-C), respectively. The modules float horizontally behind the ship until the anchor is deployed (H). Afterward, the string starts floating vertically until the ship connects its lift line (I) and begins lowering the string (K). Ultimately, the string is released (L) and descends the remaining  $\sim 5$  m to the seafloor. A complete summary of the marked events (A-L) is provided in [Section 3.4](#).

the sea. Initially, it was planned to submerge the anchor with a lift line and an acoustic release, but the harsh weather conditions did not allow this step. Afterward, the ship established a connection to the top of the string (I) to remove the extra float and attach the heavy lift line with the acoustic release. The string is gradually lowered, causing the upper float to submerge in the water (J). At this stage, the process briefly halts to attach a beacon for positioning to the lift line. Subsequently, the string commences its descent (K), maintaining a controlled speed of 0.3 m/s. Lastly, the acoustic release is activated, detaching the mooring from the lift line (L), thereby enabling the mooring to descend freely the remaining distance of less than 5 meters to reach the seafloor. During a dedicated ROV operation the string is inspected and a connection between the pathfinder and the NEPTUNE infrastructure is established, concluding the deployment process.

The logger data clearly reveals the aforementioned distinct phases of the deployment process. The provided numerical values in the following pertain to all loggers, whereas [Figure 12](#) displays a subset of three loggers chosen for clarity. The most noteworthy instances of acceleration are observed when handling the module on the deck (A-E), reaching accelerations of up to  $43.4 \frac{m}{s^2}$ . During the phase where the string is vertically floating on the sea surface, there is an extended

**Table 2:** Summary of STRAW-b measurements including readout rate, sensor type, and hosting module.

Sensor	Modules	Rate	Measurement
3-Axis Accelerometer	All Modules	0.1 Hz	continuously
3-Axis Magnetometer	All Modules	0.1 Hz	continuously
PTH <sup>1</sup>	All Modules	0.1 Hz	continuously
Powermeter <sup>2</sup> (6x)	All Modules	0.1 Hz	continuously
Temperature (3x)	All Modules	0.1 Hz	continuously
Camera	Mini- & PMT-Spec.	~1/90 Hz	continuously
Mini-Spectrometer	Mini- & PMT-Spec.	~1/90 Hz	continuously
Mini-Spectrometer <sup>3</sup>	LiDAR	2 times <sup>3</sup>	hourly
16 PMTs (ToT counts)	PMT-Spec.	1 kHz	continuously
16 SiPMs (ToT events)	Muon-Tracker	>1 GHz <sup>4</sup>	continuously
LiDAR (ToT events)	LiDAR	>1 GHz <sup>4</sup>	hourly

<sup>1</sup>PTH: Pressure-Temperature-Humidity sensor.

<sup>2</sup>The Powermeter measures each channel's current and voltage separately.

<sup>3</sup>Used for laser calibration before and after each LiDAR measurement.

<sup>4</sup>Only the events are stored. The time resolution of the TDC is below 1 ns.

period of intense acceleration, reaching levels of up to  $30.9 \frac{\text{m}}{\text{s}^2}$ . Equally strong is the acceleration seen during the anchor release (H), characterized by a singular peak reaching up to  $30.3 \frac{\text{m}}{\text{s}^2}$ . The process of lowering the string exhibits a moderate pattern, punctuated by a few brief events of up to  $22.5 \frac{\text{m}}{\text{s}^2}$  towards the end of the descent. The final drop experiences peaks at  $12.8 \frac{\text{m}}{\text{s}^2}$ , likely due to the soft seafloor. For comparison, KM3NeT adopts a bottom-up approach, with the reported maximum acceleration during the unfurling process standing at  $2.5 g_0$  ( $24.5 \frac{\text{m}}{\text{s}^2}$ ) [63]. However, the acceleration experienced during deck operations and the process of lowering the infrastructure to the sea floor is not reported.

The heeling, referring to the angle between the vertical axis and the module's orientation, indicates that it takes approximately 3 min for the line to align vertically after the anchor is released (H). The compass data shows continuous oscillations with an amplitude of up to  $15^\circ$  during the descent (K-L). On the other hand, the temperature data shows a slow decrease to  $3^\circ\text{C}$  at the seafloor, exhibiting two exponential decays as the module descends segmented into two phases (H, K-L).

#### 4 Operation of the Instruments in STRAW-b

The data acquisition (DAQ) system of STRAW-b records the data either continuously or on specific schedules. All modules contain ambient sensors to monitor the conditions inside the pressure housing, while some modules host additional sensors, as outlined in Section 2. This section presents a summary of the various measurements, while Table 2 provides a general overview, including readout rate, sensor types, and corresponding hosting modules. All recorded data from the various measurements are made accessible to the public through a database known as *Oceans 2.0*, or its more recent version, *Oceans 3.0*, as described in Section 5.2. Inside this database, files are methodically organized using data-product codes that align with the specific measurements

they represent. Subsequent sections will provide specific information regarding these data-product codes.

#### 4.1 Standardized Module

The standardized module, which each module builds on, is equipped with a 3-axis accelerometer and a 3-axis magnetometer that provide information on movement and orientation. Additionally, the module includes sensors for monitoring pressure, humidity, temperature, and power consumption within the pressure housing. The DAQ also keeps track of various software and system settings. Sensor data is collected every 10 s, while software and system settings are only saved when changes are made to reduce unnecessary data. The collected data is labeled with the data-product-code *SMRD*.

#### 4.2 Cameras, Mini-Spectrometer, and LEDs

The Mini-Spectrometer and the two PMT-Spectrometer modules contain a camera and a mini-spectrometer from Hamamatsu [20]. These sensors synchronously operate as they share the same serial peripheral interface (SPI)-bus for communicating. The camera has a readout limitation, resulting in one image and spectrum being recorded every 99.5 s. Moreover, the PMT-Spectrometer 2 captures a set of images with enabled LEDs in the neighboring module (LiDAR 2) once per hour to track its position. The measurement with enabled LEDs ceased after LiDAR 2 became unresponsive in late 2021. The LED activation and configuration information is logged by the DAQ and stored in a file with data-product-code *SMRD*. Additionally, the camera and Mini-Spectrometer each have their own files, which are labeled with data-product-codes *MSSCD* and *MSSD*, respectively.

#### 4.3 PMT-Spectrometer

The PMT-Spectrometer continuously records the PMT signals in the low precision mode of the TRB [16], which means counting ToT events rather than storing the time and duration of each event separately as described more precisely in Section 2.7. The ToT counts are stored with a frequency of 1 kHz. Once a day (around midnight UTC), a threshold scan has been conducted for the ToT, interrupting the continuous measurement for less than five minutes. The TRB is rebooted during the threshold scan. The DAQ system continuously monitors communication, and if an issue arises, it triggers a reboot of the TRB and restarts the measurement. The PMT-DAQ files, with the data-product-code *PMTSD*, rotate every hour to ensure file sizes remain below 100 MB. The utilization of PMT-Spectrometer 2 is precluded for this measurement due to a malfunctioning FPGA, which hinders the retrieval of data from the PMTs.

#### 4.4 Muon-Tracker

The Muon-Tracker utilizes the high precision mode of the TRB [16], as described in Section 2.7, to track photon detection in the scintillators with the SiPM. In this mode, all ToT events, i.e., events with timestamps and durations over the threshold, are stored. Due to the fine-tuned threshold and subsequently low background of the SiPM arrays on the scintillators, the files rotate only once a day, remaining below 100 MB, with the data-product-code *MTSD*. As with the PMT-Spectrometer, a threshold scan is performed once a day, and the DAQ system continuously monitors the TRB, triggering a restart of the measurement if needed.

## 4.5 LiDAR

The LiDARs perform various measurements, including a daily scan of the surrounding volume with the gimbal rotating over  $2\pi$ . This scan is repeated without the enabled laser to gather information on in-situ afterpulsing characteristics. A daily laser scan is also performed, where the gimbal moves in a fixed direction, and the laser changes its alignment relative to the optical axis of the detection optics. When no other measurements are ongoing, two LiDAR measurements with the enabled laser and one without the enabled laser are taken per hour. During those measurements, events are recorded for 60 s, and the gimbal points in the same direction as during the laser scan. The Laser trigger signal and the PMT's photo counting base signal are both digitized in high precision mode by the TRB, ensuring that precise time information is recorded for every Laser pulse and incoming photon. For more information about the TRB, please refer to the details provided in [Section 2.7](#). Each measurement is saved in one Hierarchical Data Format (HDF5) file identified by the data-product-code *LIDARSD*. In addition, the raw HLD files (can be multiple for a single measurement) from the TRB are stored and synchronized with the ONC database.

## 5 Distributed Control System and Data Acquisition of STRAW-b

The master control software (MCTL) operates all STRAW-b modules, except the WOM, and runs on each of them as an autonomous controller implemented as a distributed control system (DCS) [66]. Its primary goal is to ensure all sensor's safe and streamlined operation, both in manual and automated modes. To this end, the MCTL includes various functionalities such as safety control, logging, sensor operation and monitoring, bus management, inter-module communication, DAQ, and measurement execution and scheduling.

### 5.1 Data Acquisition System

The DAQ collects all sensor values and stores the data. To seamlessly integrate with the deep-sea infrastructure, a specialized software python package named SDAQ (Simple Data Acquisition) has been created and is accessible to the public [67]. This package is optimized for time series data stored in HDF5 files using lossless data compression and checksums natively supported by HDF5 [68]. The standardized file structure employed by the DAQ is illustrated in [Figure 13](#). Its purpose is to systematically arrange time series data, which are essentially sets of measurements taken over a period. Within the file, each HDF5 group is dedicated to represent a distinct time series. The primary dimension across all datasets within a group is associated with time, and each HDF5 group contains a dedicated *time* dataset to store the timestamps of the respective time series. This organization ensures uniform sizes for all datasets within a group. For extended or continuous measurements, the DAQ system initializes a file rollover after fixed periods, such as hourly or daily. In addition, metadata are stored in the attributes of the HDF5 file, group, and datasets. For example, in the context of continuous measurements, each file is assigned a unique ID, and this identifier is stored as a file attribute along with the ID of the preceding file. This approach allows for a simplified retrieval of continuous measurements at a later point in time.

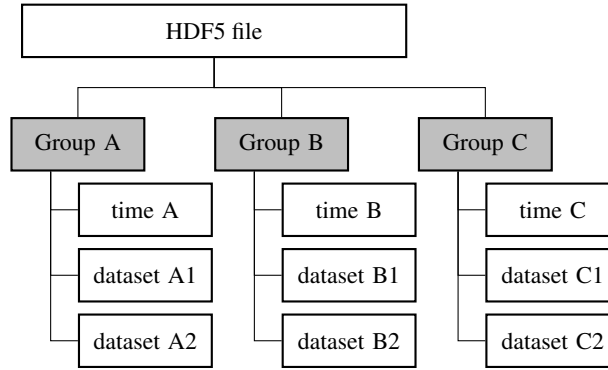


**Figure 13:** Generalized HDF5 file structure of STRAW-b’s DAQ. It exemplarily shows three data groups (A, B, C), each with two datasets and the time dataset.

## 5.2 Integration into Oceans 2.0/3.0

After recording the data on the modules, the data are downloaded and integrated into *Oceans 2.0*. *Oceans 2.0*, or its newer iteration 3.0, serves as a publicly accessible data base (DB) for all experiments connected to the ONC infrastructure. ONC manages this DB, and it can be accessed through the webpage at <https://data.oceannetworks.ca/home> or via application programming interfaces (APIs) [69]. Within this DB, files are systematically organized and labeled with data-product codes that correspond to their specific measurements. The data-product codes associated with STRAW-b are detailed in Section 4.

MCTL is equipped with an interface to ONC’s shutdown procedure in case the modules need to be powered off. In such a scenario, MCTL stops all measurements, stores the data, and puts the module in a safe state concerning software and hardware. The final shutdown command to the operating system is triggered by ONC’s shutdown procedure.

## 5.3 Communication Management

Some electronic components share a communication bus where only one member can send data at a time, such as SPI (serial peripheral interface) or I<sup>2</sup>C (Inter-Integrated Circuit). The bus-management function keeps track of all communications and distributes the available resources to prevent interference. The communication between modules depends on the utilization of the network protocol secure shell protocol (SSH) and manages measurements in cases where multiple modules are engaged. This communication holds particular significance in safeguarding sensitive PMTs from potential overexposure by adjacent LEDs. Given that the PMTs and LEDs may be situated in separate modules, the module communication system ensures that it only activates the PMTs’ high voltage (HV) while deactivating the LEDs, and vice versa.

## 5.4 Safety Control and Monitoring System

The safety control prevents any actions that potentially damage the sensors or cause data loss. For example, if an LED is activated in the same or neighboring module, the safety control will block the powering of PMTs to avoid exposing them to intense light. The logging function generates a detailed record of system events, warnings, and errors, which is essential for effective debugging,



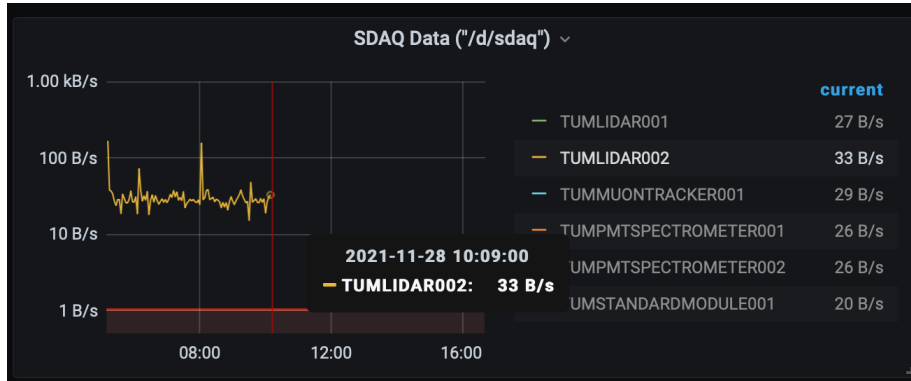


**Figure 14:** A screenshot of the real-time monitoring system based on the *TIG Stack* (Telegraf, InfluxDB, Grafana) [70, 71], displaying the last connection to the LiDAR 2 module. This system collects sensor data in real-time from various modules and allows for easy visualization and detection of any anomalies through customizable Grafana dashboards.

especially in case of rare issues. The sensor operation manages low-level functions required to operate individual sensors, while the sensor monitoring ensures their proper functioning and triggers corrective action in case of any malfunctions.

The monitoring system of each module is integrated into a real-time monitoring system for the entire detector, which uses the open-source tools Telegraf, InfluxDB, and Grafana to collect, store, and visualize sensor data in real-time [70, 71]. The combination of the tools is also called the *TIG Stack* [71]. Telegraf is used to gather data from various sources, including sensors and services, which are then sent to InfluxDB and stored as time series data.

Grafana is used to create customizable dashboards to visualize the data in real time, allowing for easy monitoring and detection of any anomalies. Additionally, the system has the ability to send alerts in real-time based on predefined thresholds, ensuring that any issues are addressed promptly [70, 71]. Figure 14 shows the last connection of the LiDAR 2 module to demonstrate the monitoring system’s performance.

## 6 A Software Package for the Data Analysis for STRAW-b

Managing and analyzing large datasets, like those generated by the STRAW-b detector, can be a challenging task. To simplify this process, a user-friendly software package called *strawb* has been developed in Python. This package provides tools for synchronizing data from ONC’s Oceans 2.0/3.0 database to a local database, as well as importing and analyzing the data. Currently, the *strawb* package repository is not public.

The *strawb* package offers several key features, such as the ability to synchronize available data from the ONC database to a local database. This feature allows users to share their code with others, with the package taking care of synchronizing the required files without downloading all files from the ONC database. By downloading only the required files, *strawb* minimizes the amount of data transfer and optimizes working with large datasets. In addition, *strawb* provides basic import functionalities for different file types, making it easy to import and process data from the STRAW-b detector. This feature reduces the time and effort required for data management. It

also includes basic and advanced analysis tools that every user can use to streamline their work with the data. These tools include functions for data visualization, quality control checks, and event selection, as well as advanced analysis techniques such as signal processing and machine learning. Additionally, *strawb* can access other sensors available on the ONC database, such as current profilers and temperature sensors. It also includes functionalities to access metadata from the ONC database, such as position information of the devices.

## 7 Summary and Outlook

As stated in this report, the successful deployment of STRAW-b was made possible by the careful development and design considerations for the 444 m-long mooring line, coupled with the deep-sea expertise of ONC. The battery-powered deployment loggers provided valuable insights into the mechanical stress experienced during the deployment. This information can be utilized for designing and testing equipment in future developments.

Furthermore, the commissioning phase of the STRAW-b project concluded in a continuous and automated detector operation for various measurements. Numerous security and monitoring mechanisms have been implemented to ensure robust and uninterrupted performance, guaranteeing high uptimes for all sensors. Notably, the DAQ system has been seamlessly integrated into ONC's Oceans 2.0/3.0 database, facilitating the availability of all collected data to the public. This integration enhances accessibility and promotes transparency, allowing researchers and interested individuals to access and utilize the valuable data collected by STRAW-b.

The planned and successful recovery of STRAW-b during the Nautilus cruise in July 2023 marks the end of the operational life of the mooring line. For the recovery, the specialized winch from the deployment was reused to coil up the wire rope, while the modules could be easily removed with the still operational click-in mechanism. Following the recovery, a thorough analysis of all instruments will be conducted to gather input for designing the detector lines of P-ONE. Preliminary visual examinations indicate that all three module failures where the connections were lost are attributed to leaking connectors on either the MJB or module side. This leakage has led to water infiltration between connectors and penetrators, ultimately resulting in salt corrosion. Additionally, biological samples from sedimentation and bio-fouling have been collected, providing supplementary data to complement the optical measurements conducted by pathfinders.

Moving forward, our primary aim involves an extensive analysis of the rich data amassed by STRAW-b, focusing on quantities directly pertinent to the functioning of P-ONE. An essential aspect under investigation is the impact of sedimentation and bio-fouling on the modules. These factors can significantly degrade the light sensitivity of the modules, which becomes especially crucial over the extended operational lifespan of P-ONE, spanning multiple decades. The data sourced from the Muon-Tracker will be harnessed to assess its potential as a calibration tool for P-ONE. Moreover, the LiDAR data offers valuable insights into water attenuation and scattering characteristics, providing a complementary perspective to the information gleaned from STRAW measurements. A noteworthy emphasis will be placed on advancing our comprehension of bioluminescence. This pursuit will encompass data analysis from the PMT-Spectrometers, cameras, and Mini-Spectrometers. Additionally, the integration of data from other deployed sensors at the

Cascadia Basin, e.g., the current meters operated by ONC, will contribute to our comprehensive understanding.

## Acknowledgments

The authors are grateful and appreciative of the support provided by Ocean Networks Canada, an initiative of the University of Victoria funded in part by the Canada Foundation for Innovation. This work is supported by the German Research Foundation through grant SFB 1258 “Neutrinos and Dark Matter in Astro- and Particle Physics” and the ORIGINS Excellence Cluster.

## References

- [1] M.G. Aartsen, R. Abbasi, M. Ackermann, J. Adams, J.A. Aguilar, M. Ahlers et al., *Evidence for neutrino emission from the nearby active galaxy NGC 1068*, *Science* **378** (2022) 538.
- [2] and R. Abbasi, M. Ackermann, J. Adams, J.A. Aguilar, M. Ahlers, M. Ahrens et al., *Observation of high-energy neutrinos from the Galactic plane*, *Science* **380** (2023) 1338.
- [3] and Mark Aartsen, M. Ackermann, J. Adams, J.A. Aguilar, M. Ahlers, M. Ahrens et al., *Neutrino emission from the direction of the blazar TXS 0506+056 prior to the IceCube-170922a alert*, *Science* **361** (2018) 147.
- [4] S. Biagi and the KM3NeT consortium, *The KM3NeT project*, *Journal of Physics: Conference Series* **375** (2012) .
- [5] G. Collaboration, A.D. Avrorin, A.V. Avrorin, V.M. Aynutdinov, R. Bannash, I.A. Belolaptikov et al., *Neutrino telescope in Lake Baikal: Present and future*, 2019.
- [6] E. Resconi, “Towards a new neutrino telescope in the Pacific Ocean.” <https://www.pacific-neutrino.org/>, 2021.
- [7] C. Barnes, M. Best, F. Johnson, L. Pautet and B. Pirenne, *Challenges, benefits and opportunities in operating cabled ocean observatories: Perspectives from NEPTUNE Canada*, in *IEEE Xplore*, pp. 1 – 7, 05, 2013, DOI.
- [8] M. Boehmer, J. Bosma, D. Brussow, L. Farmer, C. Fruck, R. Gernhäuser et al., *STRAW (STRings for absorption length in water): pathfinder for a neutrino telescope in the deep pacific ocean*, *Journal of Instrumentation* **14** (2019) P02013.
- [9] N. Bailly, J. Bedard, M. Böhmer, J. Bosma, D. Brussow, J. Cheng et al., *Two-year optical site characterization for the pacific ocean neutrino experiment (P-ONE) in the Cascadia Basin*, *The European Physical Journal C* **81** (2021) .
- [10] E.N.E.N. Harvey, *A history of luminescence from the earliest times until 1900*, Philadelphia, American Philosophical Society, 1957 (1957).
- [11] M.I. Latz, T.M. Frank and J.F. Case, *Spectral composition of bioluminescence of epipelagic organisms from the Sargasso Sea*, *Marine Biology* (1988) 441.
- [12] A. Gouveaux, *Bioluminescence of Tomopteridae species (Annelida): multidisciplinary approach*, Ph.D. thesis, Université catholique de Louvain, 08, 2016.
- [13] P.J. Herring, *The spectral characteristics of luminous marine organisms*, *Proceedings of the Royal Society of London. Series B. Biological Sciences* **220** (1983) 183 .

- [14] C. Spannfellner, *Development of pathfinder missions and instruments for the pacific ocean neutrino experiment*, Master's thesis, Technical University of Munich, 2020.
- [15] Hard Kernel, Ltd., *ODROID-C2*, 11, 2016.
- [16] A.N. et al., *TRB3: a 264 channel high precision TDC platform and its applications*, *Journal of Instrumentation* **8** (2013) C12043.
- [17] Thorlabs GmbH, *NPL Series of Nanosecond Pulsed Lasers*, 10, 2019.
- [18] Hamamatsu Photonics K.K., *Micro PMT*, 6, 2022.
- [19] C. Fink, *Development of a LIDAR system for characterizing the optical properties of seawater at Cascadian Basin*, Bachelor's thesis, Technical University of Munich, 2019.
- [20] Hamamatsu, "Mini-Spectrometer C12880MA." <https://www.hamamatsu.com/eu/en/product/optical-sensors/spectrometers/mini-spectrometer/C12880MA.html>, 2021.
- [21] E.L. Winter, *Muon tracker for the second pathfinder of the pacific ocean neutrino explorer*, Bachelor's thesis, Technical University of Munich, 2019.
- [22] Saint-Gobain Crystals, *BC-400, BC-404, BC-408, BC-412, BC-416 Premium Plastic Scintillators*, 8, 2016.
- [23] KETEK GmbH, *SiPM – Silicon Photomultiplier PM3315-WB-B0*, 12, 2018.
- [24] "Padiwa AMPS." <https://jpsc29.x-matter.uni-frankfurt.de/trbweb/?action=view&url=padiwa-amps>.
- [25] W. Kang, C. Tönnis and C. Rott, *The camera system for the IceCube Upgrade*, 2019.
- [26] Arducam, "Arducam." <https://www.arducam.com>, 2021.
- [27] L. Ruohan, *Development of STRAW-b: Strings for absorption length in water for future neutrino telescope in deep pacific ocean*, Master's thesis, Technical University of Munich, 2020.
- [28] K. Holzapfel, *Bioluminescence in the Pacific Ocean Neutrino Experiment: Shedding Light on the Deep Sea*, Ph.D. thesis, TUM School of Natural Sciences, 07, 2023.
- [29] Hamamatsu Photonics K.K., *PHOTOMULTIPLIER TUBES R1924A*, 3, 2014.
- [30] Hamamatsu Photonics K.K., *PHOTOMULTIPLIER TUBES R1925, R1925-01*, 12, 1999.
- [31] THORLABS INC., *LA1401-A N-BK7 A COAT PLANO CONVEX LENS*, 12, 2009.
- [32] E. Optics, "Hard coated OD 4.0 10nm bandpass filters." <https://www.edmundoptics.eu/f/hard-coated-od-4-10nm-bandpass-filters/13837/>.
- [33] E. Optics, "Hard coated OD 4.0 25nm bandpass filters." <https://www.edmundoptics.eu/f/hard-coated-od-4-25nm-bandpass-filters/14529/>.
- [34] E. Optics, "Hard coated OD 4.0 50nm bandpass filters." <https://www.edmundoptics.eu/f/hard-coated-od-4-50nm-bandpass-filters/14321/>.
- [35] S. Agostinelli, J. Allison, K. Amako, J. Apostolakis, H. Araujo, P. Arce et al., *Geant4—a simulation toolkit*, *Nuclear Instruments and Methods in Physics Research Section A: Accelerators, Spectrometers, Detectors and Associated Equipment* **506** (2003) 250.
- [36] J. Allison, K. Amako, J. Apostolakis, P. Arce, M. Asai, T. Aso et al., *Recent developments in geant4*, *Nuclear Instruments and Methods in Physics Research Section A: Accelerators, Spectrometers, Detectors and Associated Equipment* **835** (2016) 186.

- [37] N. Khera, *In-situ study of the ambient background at Cascadia Basin, Canada, for the Pacific Ocean Neutrino Explorer*, Master's thesis, Technical University of Munich, 2019.
- [38] "Sony commercializes the world's highest sensitivity CMOS image sensor for automotive cameras." <https://www.sony.com/en/SonyInfo/News/Press/201410/14-106E/>, 10, 2014.
- [39] Sony, *IMX225LQR*, 2014.
- [40] B.E. Bayer, *Color imaging array*, 6, 1976.
- [41] Arducam, "Arducam M12 lens kit." [https://www.arducam.com/doc/m12\\_lens\\_kit.pdf](https://www.arducam.com/doc/m12_lens_kit.pdf).
- [42] C. LED, *XLamp XP-G3 LED Data Sheet*, 2022.
- [43] LUMINUS, *SST-10-UV Product Datasheet*, 2022.
- [44] I.C. Rea, *The Pacific Ocean Neutrino Experiment: feasibility study for a new Neutrino Telescope at Cascadia Basin, NE Pacific Ocean*, Ph.D. thesis, Technical University of Munich, 2021.
- [45] B. Bastian-Querner, L.S. Binn, S. Böser, J. Brostean-Kaiser, D. Hebecker, K. Helbing et al., *The wavelength-shifting optical module*, *Sensors* **22** (2022) .
- [46] D. da Cruz and T. Jol, "Sonderforschungsbereich 42 (SFB42)." <https://sfb42.org/about>, 2020.
- [47] d.C. Diogo, H. Kilian and T. Jol, "UNDERCURRENTS." <https://sfb42.org/UNDERCURRENTS>, 2020.
- [48] V. Gewin, *How to shape a productive scientist– artist collaboration*, *Nature* (2021) .
- [49] H. Kilian and T. Jol, "Radioammonion." <https://radioammonion.net>, 2021.
- [50] "Det norske veritas rules and standards." <https://rules.dnv.com/servicedocuments/dnvpdm/>, 2023.
- [51] O.N. Canada, "Oceans 3.0, SeaTube Pro." <https://data.oceannetworks.ca/SeaTube?resourceTypeId=1000&resourceId=23543&diveId=4180&time=2020-09-11T17:45:18.000Z>, 2020.
- [52] International Organization for Standardization, *ISO 13628-6:2006 - Petroleum and natural gas industries. Design and operation of subsea production systems. Part 6: Subsea production control systems*, 2006.
- [53] C. Markou, *Km3net: Toward a cubic kilometre volume neutrino telescope in the mediterranean sea*, *Nuclear Instruments and Methods in Physics Research Section A: Accelerators, Spectrometers, Detectors and Associated Equipment* **595** (2008) 54.
- [54] A. Roberts, *The birth of high-energy neutrino astronomy: A personal history of the dumand project*, *Rev. Mod. Phys.* **64** (1992) 259.
- [55] P. Grieder, *Dumand ii: String 1 deployment, initial operation, results and system retrieval*, *Nuclear Physics B - Proceedings Supplements* **43** (1995) 145.
- [56] E. de Wolf, ed., *Technical aspects of a Very Large Volume Neutrino Telescope in the Mediterranean Sea. Proceedings, Workshop, VLVnuT Workshop, Amsterdam, Netherlands, October 5-8, 2003*, 2004.
- [57] ANTARES collaboration, *ANTARES: the first undersea neutrino telescope*, *Nucl. Instrum. Meth. A* **656** (2011) 11 [1104.1607].
- [58] G. Aggouras, E. Anassontzis, A. Ball, G. Bourlis, W. Chinowsky, E. Fahrún et al., *Nestor deep sea neutrino telescope: Deployment and results*, *Nuclear Physics B - Proceedings Supplements* **151** (2006) 279.

- [59] E. Migneco, S. Aiello, E. Amato, M. Ambriola, F. Ameli, G. Andronico et al., *Nemo: Status of the project*, *Nuclear Physics B - Proceedings Supplements* **136** (2004) 61.
- [60] M.S. Musumeci, *Construction and deployment issues for a km<sup>3</sup> underwater detector: The nemo experience*, *Nuclear Instruments and Methods in Physics Research Section A: Accelerators, Spectrometers, Detectors and Associated Equipment* **567** (2006) 545.
- [61] I. AMORE, S. AIELLO, M. AMBRIOLA, F. AMELI, M. ANGHINOLFI, A. ANZALONE et al., *Nemo: A project for a km<sup>3</sup> underwater detector for astrophysical neutrinos in the mediterranean sea*, *International Journal of Modern Physics A* **22** (2007) 3509  
[<https://doi.org/10.1142/S0217751X07037123>].
- [62] S. Adrián-Martínez, S. Aiello, F. Ameli, M. Anghinolfi, M. Ardid, G. Barbarino et al., *Long term monitoring of the optical background in the capo passero deep-sea site with the nemo tower prototype*, *The European Physical Journal C* **76** (2016) .
- [63] S. Aiello, A. Albert, S.A. Garre, Z. Aly, F. Ameli, E. Anassontzis et al., *Deep-sea deployment of the km<sup>3</sup>net neutrino telescope detection units by self-unrolling*, *Journal of Instrumentation* **15** (2020) P11027.
- [64] “Chemical-resistance-chart.” <https://www.buerkert.de/de/content/download/9318/335016/file/DEBestaendigD.pdf>, 2018.
- [65] “New hyperbaric pressure testing system at nautilus marine service.” <https://www.vitrovex.com/new-hyperbaric-pressure-testing-system-at-nautilus-marine-service/>, 2018.
- [66] T. Stout and T. Williams, *Pioneering work in the field of computer process control*, *IEEE Annals of the History of Computing* **17** (1995) 6.
- [67] H. Kilian, “A simple data acquisition (sdaq) package for python.” <https://github.com/kholzapfel/sdaq>, 2024.
- [68] T.H. group, “The HDF Group provides the feature-packed HDF5 technology suite backed by complementary supporting services..” <https://www.hdfgroup.org/>, 2021.
- [69] O.N. Canada, “Oceans 3.0 data portal.” <https://data.oceannetworks.ca>, 2020.
- [70] influxdata, “Time series data.” <https://www.influxdata.com/what-is-time-series-data/>, 2021.
- [71] influxdata, “Grafana guide. a guide to the TIG stack — Telegraf, InfluxDB, and Grafana.” <https://www.influxdata.com/grafana/>, 2021.